論文 / 著書情報
Article / Book Information

論題(和文)	熱交換器の性能解析における一般化平均温度差法
Title(English)	Generalized Mean Temperature Difference Method for Thermal Design of Heat Exchangers
著者(和文)	宇多村元昭
Authors(English)	motoaki utamura
出典(和文)	, Vol. 4, No. 1, pp. 11-31
Citation(English)	International Journal of Nuclear Energy Science and Technology, Vol. 4, No. 1, pp. 11-31
Copyright	Copyright (c) 2009 Inderscience Publishing Co. Ltd.
発行日 / Pub. date	2009, 1
DOI	http://dx.doi.org/10.1504/IJNEST.2008.017545
URL	http://www.inderscience.com/info/inarticletoc.php?jcode=ijnest&year=2008&vol=4&issue=1

A generalised mean temperature difference method for thermal design of heat exchangers

Motoaki Utamura*, Konstantin Nikitin and Yasuyoshi Kato

Tokyo Institute of Technology
2–12–1 Ookayama Meguro-ku
Tokyo 152–8552, Japan
E-mail: utamura@rccre.titech.ac.jp
E-mail: konstantin.nikitin@psi.ch
E-mail: kato@nr.titech.ac.jp
*Corresponding author

Abstract: A Generalised Mean Temperature Difference (GMTD) method instead of the Logarithmic Mean Temperature Difference (LMTD) method for heat exchangers is proposed. Unlike the LMTD method, the GMTD method allows the performance analysis of heat exchangers with distributed physical properties. GMTD is calculated by a new method to take fluid temperature profiles as a function of heat load. Mathematical proof is made that the formula of the LMTD can be derived from that of the GMTD, in the case of constant physical property. The GMTD method is applied to experiments of a hot water supplier with supercritical carbon dioxide as a heating media that works through its pseudo-critical point where specific heat behaves anomaly. The empirical correlations of the local Nusselt number and pressure loss coefficient based on the GMTD gives an accurate prediction of the overall heat transfer coefficient, with a 5% error rating, whilst an error two times larger appears in the case of the LMTD.

As an anomaly or abnormally?

Keywords: Logarithmic Mean Temperature Difference (LMTD) method; Generalised Mean Temperature Difference (GMTD) method; Overall Heat Transfer Coefficient; OHTC; supercritical carbon dioxide; heat exchanger; Nusselt number.

Reference to this paper should be made as follows: Utamura, M., Nikitin, K. and Kato, Y. (xxxx) 'A generalised mean temperature difference method for thermal design of heat exchangers', *Int. J. Nuclear Energy Science and Technology*, Vol. X, No. Y, pp.000–000.

Biographical notes: Motoaki Utamura is a Visiting Professor of the Tokyo Institute of Technology (Tokyo Tech), a registered Professional Engineer of Japan, a biographee in *Marquis Who's Who in the World*, a member of the American Society of Mechanical Engineers, and inventor and patent holder of the 'Inlet Fogging' gas has turbine power augmentation technology, widely practised in the world. He has worked in nuclear safety research and now works in solar thermal research, including optics to thermal cycle, especially research on novel gas turbines using supercritical CO_2 as a working fluid, and biomass power generation. He has published more than 50 scientific papers, two books and more than 50 patents.

Konstantin Nikitin obtained his MSc at MEPhI in 1993 and his PhD at Tokyo Tech in 2001. His previous research topics include transient analyses of nuclear reactors and nonproliferation aspects. He is currently doing a thermohydraulic study for microchannel heat exchangers in the gas turbine cycle.

Yasuyoshi Kato is a Professor of the Research Laboratory for Nuclear Reactors at Tokyo Tech. He worked on developing Fast Reactors (FRs) in Hitachi Ltd. for 28 years from 1971, and moved to Tokyo Tech in 1999. He has proposed an Advanced Nuclear Energy System (ANES) with trigeneration of electricity, heat, and methane and methanol; and for AES, he has developed next-generation Supercritical Carbon Dioxide (S-CO_2) gas turbine FR systems, S-CO_2 cycle Waste Heat Recovery Systems (WHRS) from power plants, and Microchannel Compact Heat Exchangers (MCHEs) for the S-CO_2 systems. He has published papers on reactor physics, advanced FR and high-temperature gas-cooled reactor systems, WHRs, ANES and MCHEs. He has written books on advanced small nuclear reactor systems and cellular automata.

1 Introduction

The compactness and efficiency improvement of heat exchangers are important, particularly for cost reduction, in all energy systems: heat pumps, refrigeration and waste heat recovery systems for a variety of residential, industrial, automotive and process industry applications. The Logarithmic Mean Temperature Difference (LMTD) method (Hesselgreaves, 2001) has been a key concept to measure compactness, as shown in the Colburn *j* factor, given as:

$$j = \frac{D_h}{4L} Pr^{2/3} N \tag{1}$$

where $N = NTU$ (Number of Thermal Units), and assuming $K_1 \le K_2$:

$$N = (T_i^1 - T_0^1)/\Delta T_{LMTD}. \tag{2}$$

As shown in later sections, the application of the LMTD method is limited to a heat exchanger system containing fluid with constant physical properties. Therefore, ΔT_{LMTD} in Equation (2) should be modified where physical properties are not constant.

On the other hand, as an energy-saving tactics that reduces carbon dioxide emission in the air, a supercritical CO_2 cycle is likely to be adopted because of the advancement in turbomachinery technology (Utamura and Tamaura, 2006). For example, electrically driven hot water suppliers that use supercritical CO_2 as a heating medium tend to be widely introduced. This is because the have a higher COP, as well as a nontoxic and nonartificial nature. The hot water supplier operates under conditions that include the pseudocritical point of CO_2. It is because the thermodynamic state of CO_2 is selected so as to minimise the work of the compressor in the cycle. The physical properties there are quite sensitive to temperature changes, and are thus far from having a constant nature. Thus, rigorous analysis of the performance of the hot water supplier requires the introduction of new methodology instead of using the LMTD method. The purpose of this study is to derive a Generalised Mean Temperature Difference (GMTD) method and show its validity by applying it to an experiment of the hot water supplier using supercritical CO_2 and water as heating media.

2 Theory

2.1 Derivation and limitation of LMTD

For the counterflow heat exchangers in Figure 1, the temperature profiles of two fluids obey the following governing equations:

$$\begin{aligned} m_1 Cp_1(x)\frac{dT_1}{dx} &= -a_1 U_1(x)(T_1 - T_2) \\ m_2 Cp_2(x)\frac{dT_2}{dx} &= -a_2 U_2(x)(T_1 - T_2) \end{aligned} \tag{3}$$

where:

$$a_1 U_1(x) = a_2 U_2(x) = c(x)$$
$$a_i = A_i / L.$$

Figure 1 Variation of the fluid temperatures in a counterflow heat exchanger

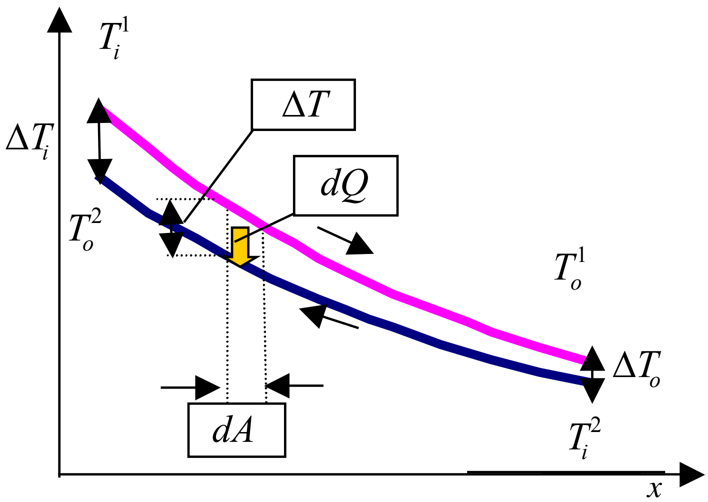

For parallel-flow configuration, m_2 in Equation (3) should be replaced by $-m_2$. From Equation (3), the following equation can be reduced:

$$K_1(x)K_2(x)\frac{d\Delta T}{dx} = c(x)(K_1(x) - K_2(x))\Delta T(x) \tag{4}$$

where:

$$\Delta T(x) = T_1(x) - T_2(x)$$
$$K_i(x) = m_i Cp_i(x).$$

Provided that K_i, c are constants, the analytical integration of Equation (4) can be executed, yielding:

$$\Delta T(x) = \Delta T_i e^{\gamma x}$$

and

$$\Delta T_0 = \Delta T_i e^{\gamma L} \tag{5}$$

where:

$$\gamma \equiv c\left(\frac{1}{K_2} - \frac{1}{K_1}\right)$$

$$K_i = m_i Cp_i.$$

Noting:

$$Q_0 = K_1(T_1^i - T_1^0) = K_2(T_2^0 - T_2^i) \tag{6}$$

then:

$$\Delta T_0 - \Delta T_i = Q_0\left(\frac{1}{K_2} - \frac{1}{K_1}\right) = \frac{\gamma Q_0}{c}.$$

From Equations (5) and (6):

$$\ln\frac{\Delta T_0}{\Delta T_i} = \gamma L = \frac{C^*}{Q_0}(\Delta T_0 - \Delta T_i). \tag{7}$$

We define ΔT_{LMTD} as:

$$\Delta T_{LMTD} = \frac{\Delta T_0 - \Delta T_i}{\ln\dfrac{\Delta T_0}{\Delta T_i}}. \tag{8}$$

From Equation (7), we have:

$$Q_0 = A_i U_i \Delta T_{LMTD} = C^* \Delta T_{LMTD}. \tag{9}$$

For example, by use of Equation (9) one could obtain an Overall Heat Transfer Coefficient (OHTC) U_i from measurements.

2.2 *Temperature difference as function of heat load Q*

For an infinitesimal segment of a heat exchanger, the following equation holds:

$$\begin{aligned} dQ &= U_i dA_i \Delta T \\ dA_i &= \frac{A_i}{L}dx. \end{aligned} \tag{10}$$

In the case of constant physical properties, using the temperature difference between fluids at both ends, Equation (5) can be alternatively expressed by:

$$\Delta T = \Delta T_i e^{\frac{x}{L} ln \frac{\Delta T_0}{\Delta T_i}}. \tag{5$'$}$$

The integration of Equation (10) using Equation (5)′ gives the relation between heat load Q and length x as:

$$Q = \frac{c\Delta T_i}{\ln \frac{\Delta T_0}{\Delta T_i}} \left(e^{\frac{x}{L} ln \frac{\Delta T_0}{\Delta T_i}} - 1 \right) \tag{11}$$

at $x = L$

$$\frac{\Delta T_0}{\Delta T_i} = \frac{\ln \frac{\Delta T_0}{\Delta T_i}}{c\Delta T_i} Q_0 + 1. \tag{12}$$

By use of Equation (12), Equation (11) can be rewritten as:

$$\frac{Q}{Q_0} = \frac{e^{\frac{x}{L} ln \frac{\Delta T_0}{\Delta T_i}} - 1}{\frac{\Delta T_0}{\Delta T_i} - 1}. \tag{11$'$}$$

The application of Equation (11)′ to Equation (5)′ gives ΔT as a function of Q:

$$\Delta T = \Delta T_i \left[\left(\frac{\Delta T_0}{\Delta T_i} - 1 \right) \frac{Q}{Q_0} + 1 \right]. \tag{13}$$

It is seen that ΔT is a linear function of Q in the case of constant physical properties.

2.3 GMTD method for variable physical properties

The integration of Equation (10) over an entire heat exchanger gives:

$$\int_0^{Q_0} \frac{dQ}{\Delta T(Q)} = \int_0^{A_i} U_i dA_i. \tag{14}$$

If we define the GMTD $\Delta \overline{T}$ and averaged overall heat transfer coefficient $\overline{U}_i$ by:

$$\begin{aligned} \frac{1}{\Delta \overline{T}} &\equiv \frac{1}{Q_0} \int_0^{Q_0} \frac{dQ}{\Delta T(Q)} \\ \overline{U}_i &\equiv \frac{1}{A_i} \int_0^{A_i} U_i dA_i \end{aligned} \tag{15}$$

then, similar to Equation (9), from Equation (14) we have:

$$Q_0 = A_i \overline{U}_i \Delta \overline{T} = \overline{C}^* \Delta \overline{T}. \tag{16}$$

Given $Q_0, A_i, \Delta\overline{T}$ prior to, for example, experiments or design condition, Equation (16) gives an Averaged Overall Heat Transfer Coefficient (AOHTC) $\overline{U}_i$. Also, with Q_0, $\overline{U}_i$, $\Delta\overline{T}$ given, one can determine heat transfer area A_i and the size of the heat exchanger. Equation (2) may also be modified as:

$$N = (T_i^1 - T_0^1)/\Delta\overline{T}. \tag{2$'$}$$

One can execute numerical integration of the first equation of Equation (15) and evaluate $\Delta\overline{T}$, provided that the heat duty Q_0 and inlet temperatures T_i^1 and T_i^2 of both fluids are given. In the case that U_i is constant, clearly $\overline{U}_i$ and $\Delta\overline{T}$ are exactly equal to U_i and ΔT_{LMTD}, respectively.

Using Equation (15):

$$\begin{aligned}\frac{1}{\Delta\overline{T}} &= \frac{1}{Q_0}\int_0^{Q_0} \frac{dQ}{\Delta T(Q)} \\ &= \frac{1}{\Delta T_i}\frac{1}{\frac{\Delta T_0}{\Delta T_i}-1}\ln\left[\left(\frac{\Delta T_0}{\Delta T_i}-1\right)\frac{Q}{Q_0}+1\right]_0^{Q_0}.\end{aligned} \tag{17}$$

This leads to:

$$\Delta\overline{T} = \frac{\Delta T_0 - \Delta T_i}{ln\frac{\Delta T_0}{\Delta T_i}} = \Delta T_{LMTD}. \tag{18}$$

3 Numerical calculation

3.1 Numerical procedure

Given $Q_0, T_i^1, T_i^2, m_1, m_2, P_i^1$ and P_i^2, the temperature profiles of both fluids and resultant temperature difference profile may be obtained as follows. Calculating specific enthalpies at inlets, one can obtain the specific enthalpy and temperature of cold-side fluid (indicated by Suffix 2) at the outlet. Next, heat duty Q_0 is expressed by a sum of M sets of heat segment $q(=Q/M)$, each of which is sequentially numbered from the hot-side fluid entry. Figure 1 shows the calculation procedure, which starts from the first segment. Enthalpies and temperatures at the node on the right edge of the segment are obtained from the heat balance and thermodynamic state equation. The thermodynamic state of each fluid was calculated by PROPATH (Ito *et al*., 1990) in this study. As the node on the right edge of the segment shares the node on the left edge of the next segment, calculation proceeds in sequence until the heat load reaches the heat duty given. At each node, the temperature difference of two fluids is calculated. Thus:

$$\int_0^{Q_0} \frac{dQ}{\Delta T(Q)} = \sum_{j=1}^{M} 2q/(\Delta T_j + \Delta T_{j+1}) \tag{19}$$

and

$$\Delta\overline{T} = M \Big/ \sum_{j=1}^{M} 2 \big/ (\Delta T_j + \Delta T_{j+1}). \tag{20}$$

3.2 Numerical example

3.2.1 Constant physical property

Figure 2 shows the temperature difference profile using Equation (13), with $\Delta T_i = 28$, $\Delta T_0 = 9$, $Q_0 = 4.6\ kW$ under constant physical properties. Mean temperature difference by the LMTD method gives 16.7 K, and the pinch point appears at the entry of the cold fluid.

Figure 2 Temperature difference profile under constant physical property

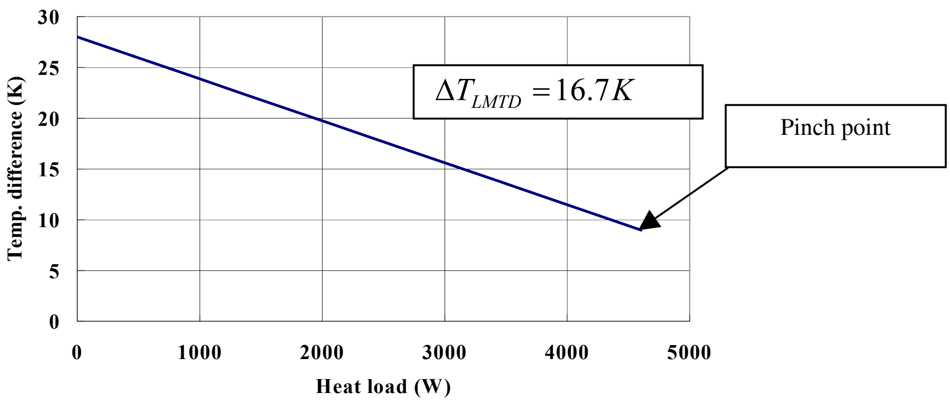

3.2.2 Distributed physical property

With the same input as above, the pseudocritical state of carbon dioxide and water were considered as heating media. Figures 3, 4 and 5 show physical property variations, temperature profile and a variation of temperature difference between two fluids expected in hot water suppliers. Physical properties were calculated by PROPATH (Ito *et al.*, 1990). The Pinch point appears in the middle of the heat exchanger where specific heat is at maximum at the pseudocritical point of carbon dioxide. The critical point exists at 7.4 Mpa and 303 K. Equation (20) gives $\Delta T_{LMTD} = 167\text{ K} \rightarrow \Delta\overline{T} = 9.6\text{ K}$ due to the nonlinear characteristics of physical properties. Averaged heat conductance $\overline{C}^*$ was evaluated to be 480 W/K.

Please rewrite the highlighted text to make its meaning clear.

Figure 3 Behaviour of physical property of carbon dioxide in pseudocritical state

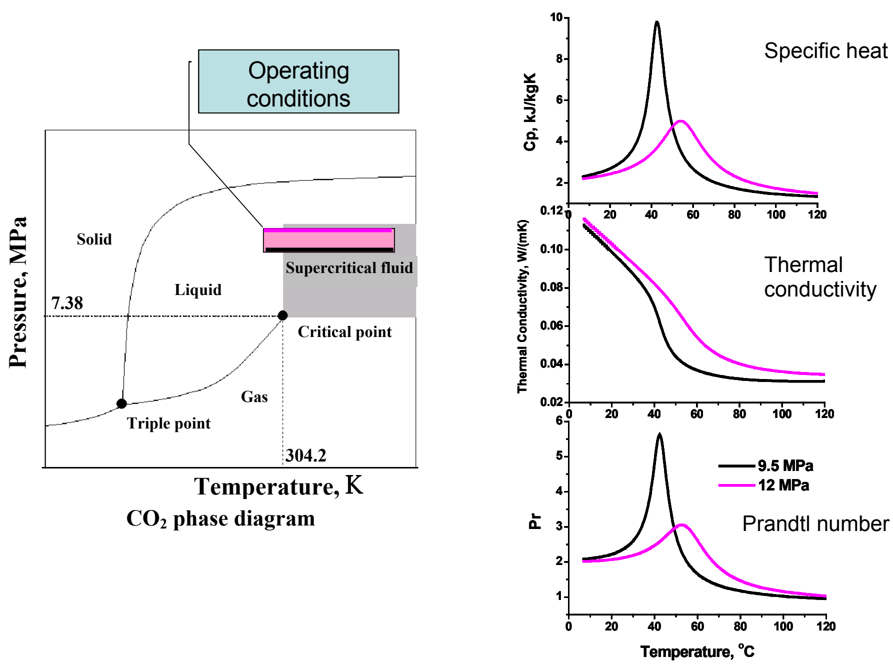

Figure 4 Temperature profile in heat exchanger with distributed physical property

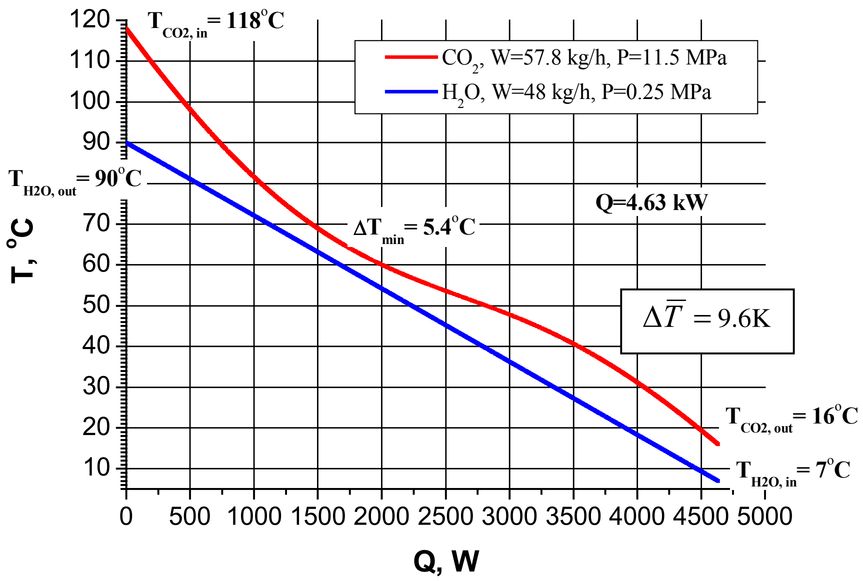

Figure 5 Temperature difference profile reduced from Figure 4

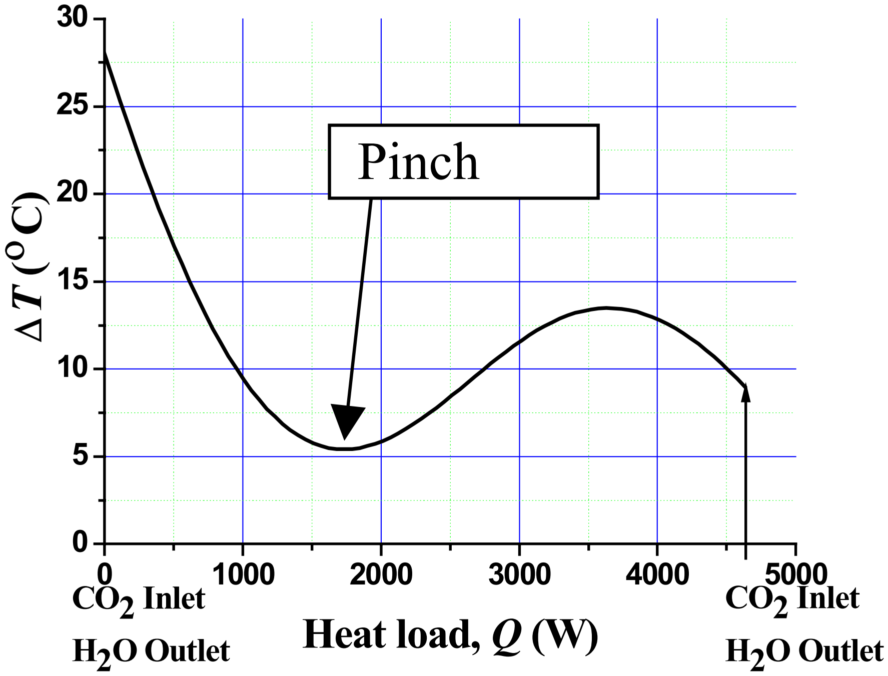

This implies that a heat transfer area 1/0.58 = 1.73 times larger than those predicted by the LMTD method is actually needed, which differentiates between the present methodology and the LMTD method.

3.2.3 Limitation of heat exchange rate

In terms of temperature profile as a function of heat load, Figure 6 shows an example of an impossible temperature profile in practice. This method, in turn, shows where the limitation of heat exchange capacity is, and suggests countermeasures for it. With the given flow rates, 17ºC inlet water temperature cannot produce hot water of 65ºC. It comes from the huge specific heat of carbon dioxide at the state quite near the critical pressure (P = 7.4 Mpa, see Figure 3). Analysis indicates that an inlet water temperature of 54ºC, at least, should be prepared to obtain hot water of 65ºC at the exit, and the resultant heat duty available will be limited to 1500 W, with the temperature difference between the two fluids becoming zero. Thus, owing to the method, an operable range could be known without physical dimensions and OHTC. The design heat duty of 6.02 kW is not attainable under the pressure condition of 8 MPa.

Figure 6 Operability and heat exchange capability

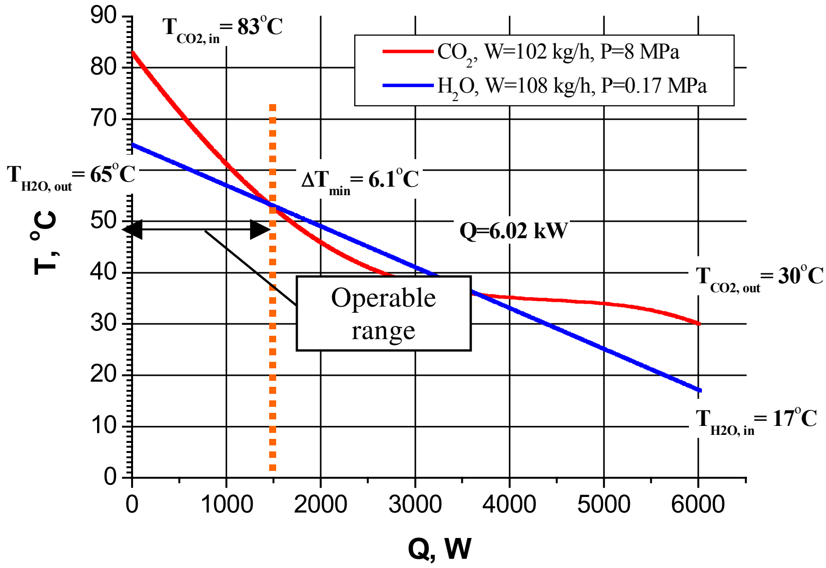

4 Verification by experiment

In order to demonstrate the validity of the present methodology (GMTD), experiments were carried out to derive empirical correlations for the Nusselt number and the pressure loss factor for hot water suppliers using supercritical carbon dioxide and water as heating media.

4.1 Experimental facility

A schematic diagram of the experimental loop is shown in Figure 7. Carbon dioxide from the low-pressure tank is compressed by the oil compressor. High-pressure gas is heated by Electric Heater 1 (1.9 kW) before passing through Gas Cooler 1 and after the oil separators. The resulting CO_2 is forwarded through a turbine-type flow meter to the inlet of the test section, where the Microchannel Heat Exchanger (MCHE) is installed. A description of MCHE can be found elsewhere (Tsuzuki *et al*., 2005). The pressure of CO_2 gas discharged from the MCHE outlet is reduced by a flow rate control expansion valve and transferred to Electric Heater 2 (2.2 kW). CO_2 gas is heated by Electric Heater 2 (2.2 kW) in order to maintain the CO_2 in the gas phase. Because of the adiabatic expansion process, the pressure of CO_2 is lowered, so the temperature becomes saturated. After heating by Heater 2, the CO_2 gas temperature is adjusted by Gas Cooler 2 for CO_2 gas to obtain a suitable temperature before returning to the CO_2 low-pressure tank. The flow meter of the CO_2 side is installed just after Gas Cooler 2. The city water is directly supplied to the H_2O-side inlet; the city water temperature can be adjusted using the chiller/warmer to meet the required testing conditions.

Figure 7 Flow diagram of supercritical CO_2 experimental loop

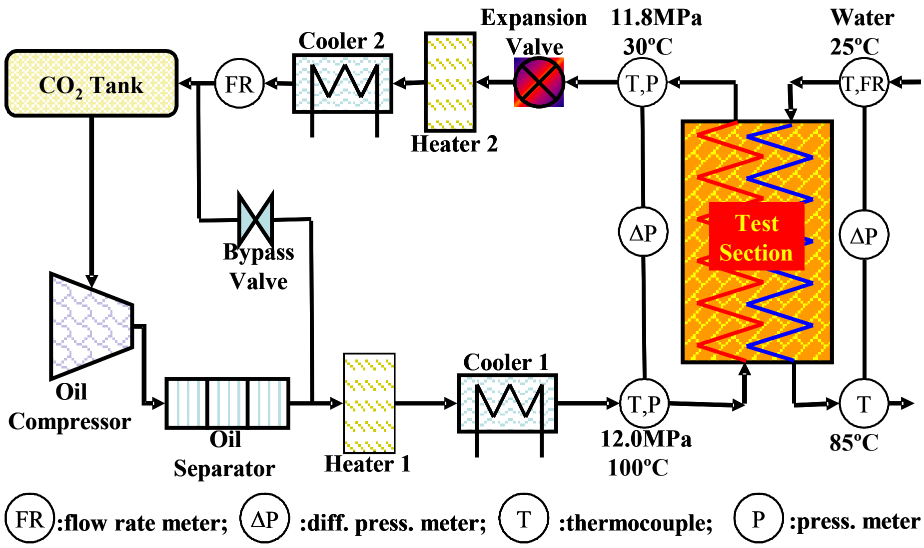

The experimental procedure is as follows: While the water inlet pressure is not controlled (~0.2–0.3 MPa), the CO_2 inlet pressure is controlled by the compressor and bypass valve. The CO_2 inlet temperature is controlled by Heater 1 and Cooler 1, and the water inlet temperature by an additional heater/cooler (not shown). The water outlet temperature is controlled by the water flow rate control system (not shown). The CO_2 flow rate is controlled by the CO_2 flow rate control system (not shown). Only the CO_2 flow rate is varied during the experiment. The water flow rate is obtained as a result of water outlet temperature control.

The experimental facility requires about three hours to reach a steady-state condition from the beginning of an experimental run. When some parameters are changed (*e.g.*, a flow rate), it requires 30 min to approach a new steady-state condition. A steady-state condition was determined as the condition when the fluctuation of measured parameters is well within the range of measurement accuracy for at least 10 min. The CO_2 and H_2O temperatures, pressures and pressure drops were directly measured and used in further calculations, while the flow rate value was corrected according to the measured CO_2 temperature and pressure near the location of the flow meter. The corrective dependencies were provided by the manufacturer of the experimental loop. All the values were then averaged over 5 min intervals. Throughout the day of the experiment the inlet pressure and temperature of hot/cold sides were kept constant, while the set value of the flow rate was changed in 5 kg/h increments.

The MCHE was manufactured from three flat copper plates that have fluid flow passages chemically milled into them. This technique is similar to that used in the manufacturing of electronically printed circuit boards. The plates are then diffusion bonded together into blocks to form a heat exchanger core of the required capacity.

The new MCHE has core dimensions of 870 × 78 × 14 mm, as shown in Figure 8. This MCHE includes one H_2O and two CO_2 plates combined in a sandwich structure, called double banking. The hot side and cold side fluid are CO_2 and water, respectively. The flow direction of fluids is countercurrent.

Figure 8 Configuration of MCHE

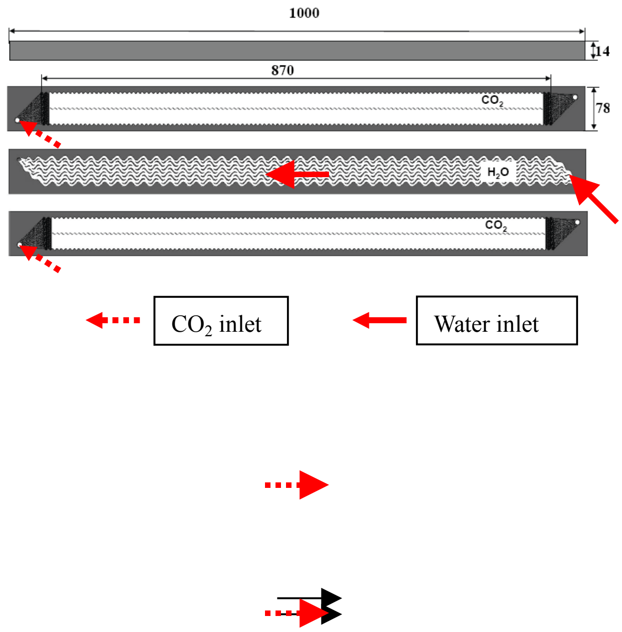

4.2 Instrumentation

The CO_2 inlet pressure of the MCHE was measured using a pressure gauge transducer with an accuracy of ±0.25% over the full range of 13 MPa. The pressure drop was measured using a differential pressure gauge, with an accuracy of ±0.15% over the full range of 400 kPa for the CO_2 side and 50 kPa for the H_2O side. The T-type (Copper/Constantan) thermocouples with an accuracy of ±0.5°C at the range of 40°C –125°C were used for temperature measurement on both the cold and hot side. Thermocouples were inserted into the inlet and outlet of the MCHE's distributors. All thermocouples were calibrated at water boiling and freezing points. The CO_2 flow meter accuracy was ±5% over the full range of 20–88 kg/h.

All measurements were recorded automatically with a 0.5 Hz sampling frequency.

4.3 Experimental conditions

The inlet temperature of the CO_2 side is set at about 100°C to 118°C, while the pressure reaches up to 11.0 to 12.5 MPa. This hot supercritical CO_2 heats up the city water from 7°C or 25°C to 85°C, 90°C or 95°C throughout the new MCHE or double tube heat exchanger. The city water's pressure is estimated at 0.25 MPa. The outlet temperature of the CO_2 side or the flow rate of H_2O is the dependent parameter, resulting from heat exchange in test sections. More than 50 test cases were run. Those experimental conditions are clearly given in Table 1. It should be noted that both the Reynolds number and Prandtl number vary not only among test runs, but also within the heat exchanger.

Please provide heading for column 1.

Table 1 Experimental conditions

	CO_2 side		*Water side*	
	Min	*Max*	*Min*	*Max*
Press. (Mpa)	9.5	12.6	~0.25	
Flow rate (kg/h)	26.8	81.1	17.4	50.4
Temp. (deg C)				
inlet	99.2	120.4	4.3	27.6
outlet	19.4	45.6	84.9	93.4
Heat load (W)	1604	4628	1604	4628
Reynolds no.				
inlet	7351	19773	110	587
outlet	1832	9960	510	1627
Prandtl no.				
inlet	1.03	1.05	5.74	11.43
outlet	2.06	2.89	1.89	2.10

4.4 Correlation for Nusselt number

An empirical formula of the local Nusselt number was obtained based on the GMTD method.

Two assumptions were made:

1 The same equation can be applied to both fluids, because the central part of the flow channel of MCHE is geometrically similar between both flow channels ends.

2 It is possible to express the Nusselt number as the product of polynomials of the Reynolds and Prandtl numbers as:

$$Nu = C_1 \times Re^m Pr^n. \tag{21}$$

Heat conductance may be expressed by:

$$C^* = U_2 A_2 = 1 \Big/ \left(\frac{1}{\alpha_1 A_1} + \frac{\Delta t_w}{\lambda A_w} + \frac{1}{\alpha_2 A_2} \right), \tag{22}$$

where heat transfer coefficient α is related to Nu as $\alpha = \dfrac{\lambda Nu}{D_h}$ from the definition of the Nusselt number.

In Equation (22), the product of $\Delta t_w / \lambda A_w$ is a hundred times less than the other terms, and was neglected since the conductivity of copper is 387 W/(mK) with the wall thickness of MCHE at about 0.5 mm. Then, by substituting Equation (21) into Equation (22) and using Assumption 1, we have:

$$U_2 = \frac{C_1 A_1 \lambda_2 \lambda_1 Re_1^m Pr_1^n Re_2^m Pr_2^n}{D_h^1 A_2 \lambda_2 Re_2^m Pr_2^n + D_h^2 A_1 \lambda_1 Re_1^m Pr_1^n} \equiv C_1 F. \tag{23}$$

Note that C_1 here is similar to that in Equation (21). Local physical properties F and U_2 can be calculated based on local bulk temperature and fluid pressure. To this end, they should be functions of heat load. Using Equations (15) and (23), the calculation of AOHTC was numerically executed by changes in variables:

$$\overline{U}_i^{calc.} = \frac{1}{A_i}\int U_i dA_i = \frac{1}{A_i}\int U_i(Q)\frac{dA_i}{dQ}dQ \cong \frac{1}{Q_0}\int U_i(Q)\frac{\Delta\overline{T}}{\Delta T(Q)}dQ = \frac{C_1}{M}\sum_{j=1}^{M} F_j\frac{\Delta\overline{T}}{\Delta T_j} \equiv C_1\overline{F}. \quad (24)$$

Provided that power indices m and n in Equation (21) are previously determined, then $\overline{F}$ can be calculated and constant C_1 may be obtained by application of the least squares method. For the determination of m and n, refer to Utamura *et al*. (2006). The number of subdivisions M of the heat exchanger was typically 1000. It is important to note that thermal parameters should be expressed by heat load in order to evaluate local properties.

4.5 Pressure loss coefficient

Pressure loss behaviour is closely related to heat transfer characteristics, in the case of variable physical properties. Once the correlation for the Nusselt number is obtained, then with the help of Equation (10), pressure loss may be numerically calculated by the change in the independent variable from length to heat load as:

$$\begin{aligned} &\Delta P = \int_0^L \varphi dx = \int_0^{Q_0} \varphi\frac{dx}{dQ}dQ = \int_0^{Q_0}\varphi\frac{dQ}{c\Delta T} \\ &\varphi \equiv fG^2/2\rho D_h. \end{aligned} \quad (25)$$

Here, the functional form of $f = C_2 Re^{-r}$ was assumed for the CO_2 side. C_2 and r were best fitted against pressure drop measurements by means of the least squares method. Thus, hydraulic characteristics are closely connected to thermal characteristics in a heat exchange system of variable physical property.

5 Discussions

5.1 Thermal performance

5.1.1 Comparison of GMTD method with LMTD method

The literature shows that the power index of Reynolds number 0.8 is applicable to a variety of fluids.

The parametric study was done for the power index of the Prandtl number ranging from 0 to 0.8. It was found that $Pr^{0.6}$ gives the best fit for the FLUENT calculation for MCHE. Therefore, the Nusselt number formula can finally be obtained in the following form:

$$Nu = C_1 \times Re^{0.8} Pr^{0.6}. \quad (26)$$

Figure 9 shows the results. The axis shows measured $\overline{U}_i$(AOHTC) reduced by Equation (16), and abscissa calculated by Equations (23) and (26). Both were based on the hot-side (carbon dioxide side) heat transfer area, as the whole data are correlated in line and Assumption 1 in Section 4.4 was proved. The best fit value of C_1 for PCHE-M(MCHE) gives $C_1 = 0.0473$ in Equation (26). Prediction error by the present correlation applied to MCHE was 5%. Shown in Figure 10 regarding mean temperature difference, LMTD is ~2 times larger than GMTD. This implies that LMTD may give a smaller heat transfer area in the present case. Figure 11 shows averaged heat conductance. It is clearly demonstrated that the GMTD method gives an excellent correlation with a small prediction error, while the LMTD method gives a poor result.

Figure 9 Relation of $\overline{U}^{exp}$ and $\overline{F}$

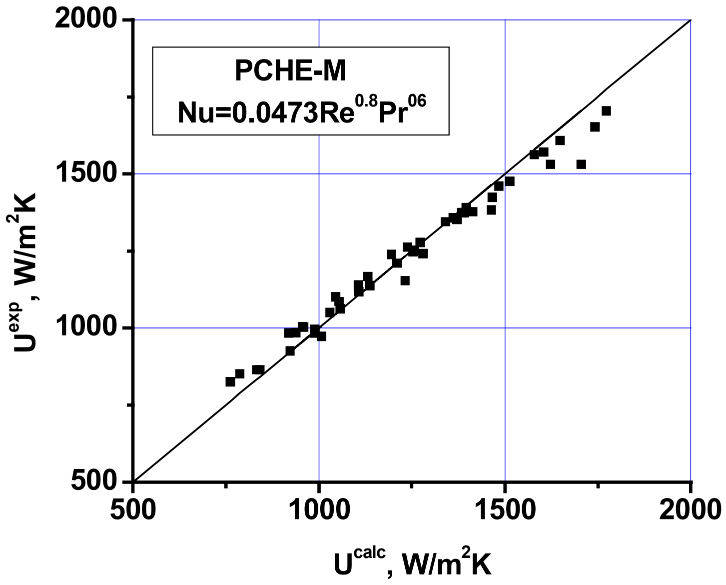

Figure 10 Comparison of GMTD and LMTD

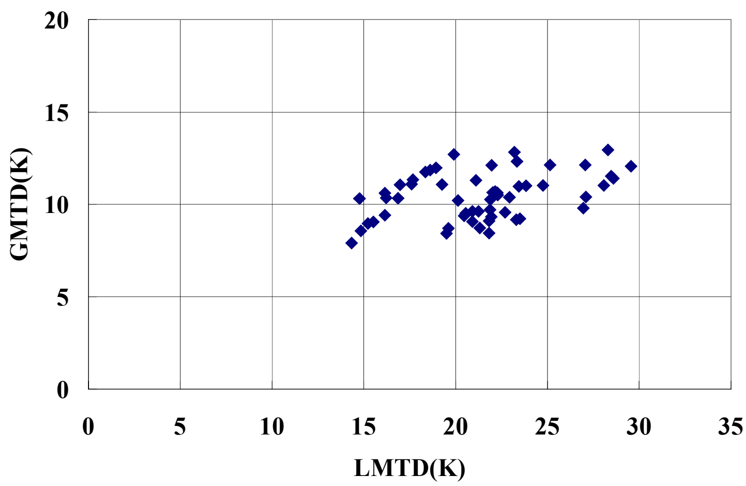

Figure 11 Heat conductance by two methods

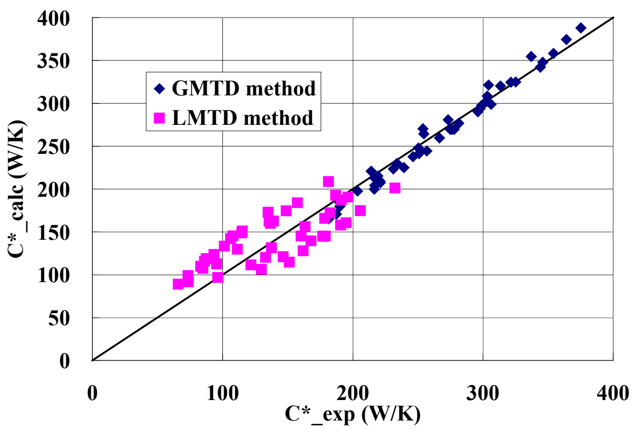

5.1.2 Comparison of reproduced temperature with measured one

Figure 12 compares measured temperatures along the heat exchanger length with the reproduced temperature profile using Equation (26) with $C_1 = 0.0473$. 'Cold' means water and 'hot' means CO_2. Excellent agreement was obtained in the entire region of MCHE. The length was calculated by applying the overall heat transfer coefficient and heat transfer area per length step by step in the heat load segment.

Figure 12 Predicted and measured temperature profile in MCHE

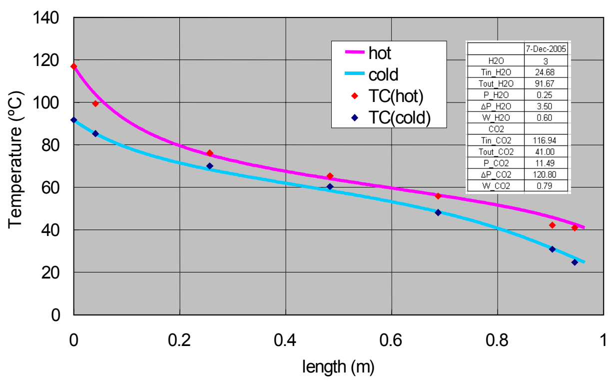

Four data plots at right and left ends of two curves exhibit fluid temperatures measured at inlet and exit plenums whose locations are indicated by arrows in Figure 8.

Similarly, Figure 13 exhibits calculated profiles of the OHTC and heat transfer coefficient of both fluids. Significant profiles of heat transfer coefficients were observed as anticipated. It is also seen that heat transfer rate is governed by the water-side heat transfer coefficient, which comes from a bigger hydraulic channel diameter. Also, the overall heat transfer coefficient U is seen to have a large distribution in the heat exchanger tested.

Figure 13 Calculated profile of OHTC and HTC in MCHE

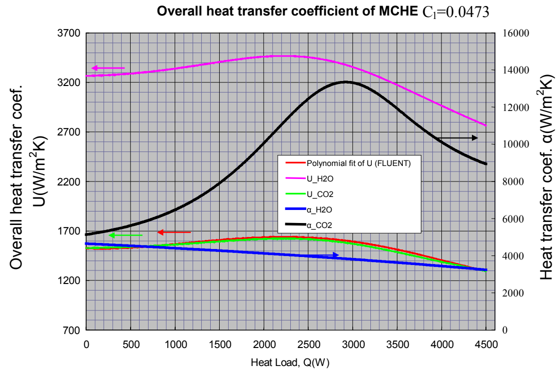

5.2 Hydraulic performance

From the Coefficient of Performance (COP) point of view, a pressure drop in the CO_2 side is important. Figure 14 attempts to correlate pressure loss measured at the hot side in terms of the Reynolds number averaged over an entire heat exchanger (MCHE). Data are seen as scattered due to the fact that the Reynolds number also has a big profile in the heat exchanger caused by the variation of dynamic viscosity. Next, with the help of Equation (25), where local pressure loss influenced by heat transfer effect was taken into account, parametric studies were carried out. The functional form of pressure loss coefficient $f = C_2 Re^{-r}$ was assumed and unknown parameters C_2 and r were determined so that the calculation fit the measured data best. Figure 15 shows the result with $C_2 = 2.294$ and $r = 0.25$. An excellent prediction was obtained, unlike in Figure 14. Prediction error was within 5% for MCHE because the local heat transfer effect, *i.e.*, the distribution of the product of $c\Delta T$, is taken into account in Equation (25). Coincidentally, the same value of power as in the Blasius formula was obtained.

Figure 14 Pressure loss correlated with averaged *Re*

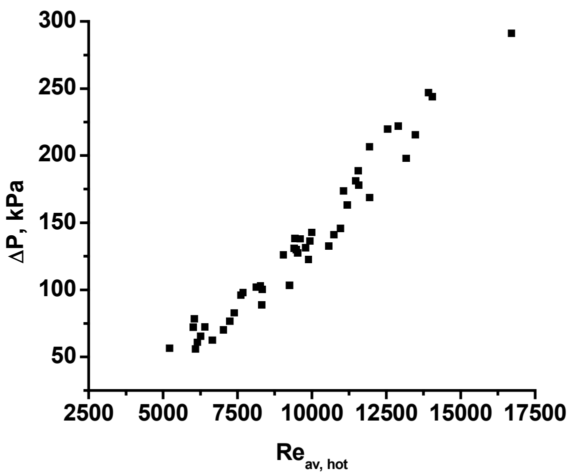

Figure 15 Comparison of calculation with experiment

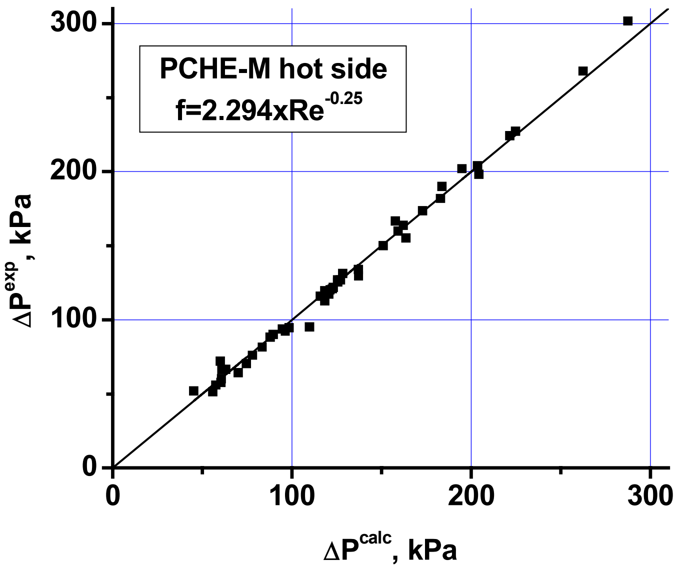

Figure 16 Design flow diagram for heat exchangers with distributed physical properties

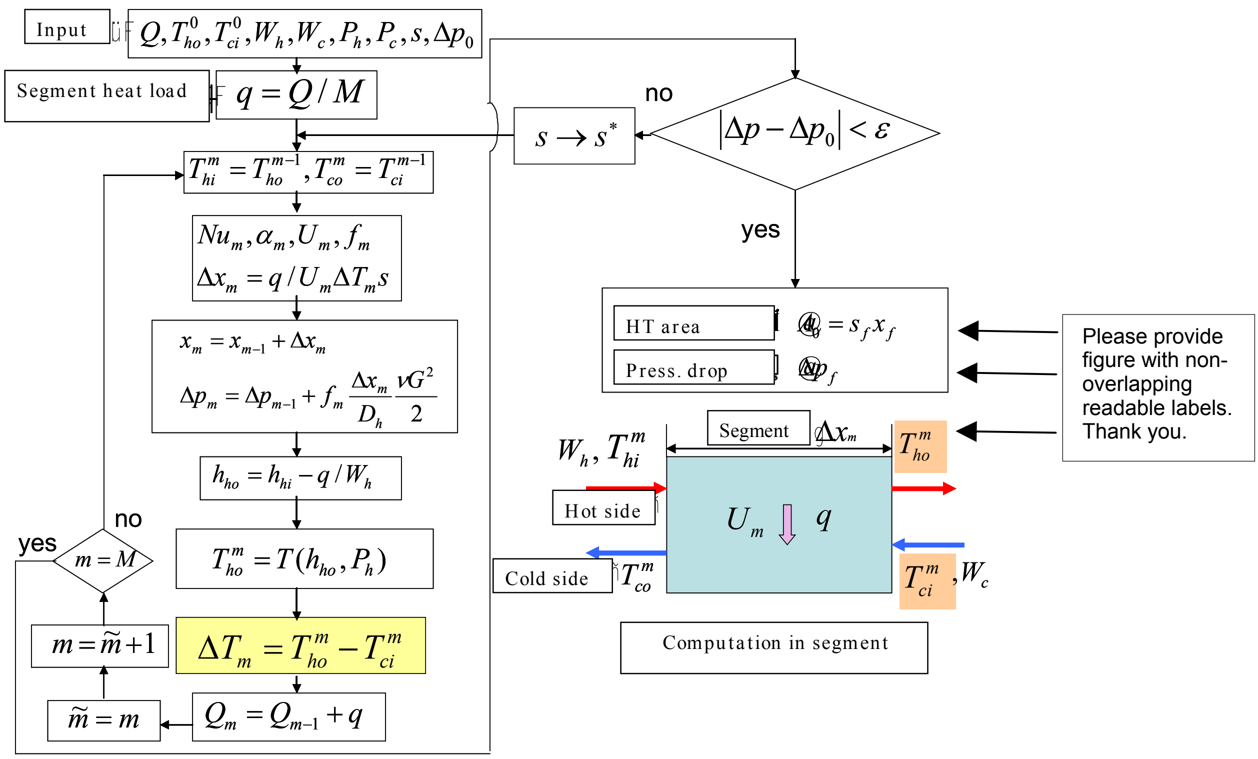

5.3 Design flow diagram using GMTD method

A design flow diagram for heat exchangers with variable physical properties is shown in Figure 16. For a given heat duty, inlet conditions, mass flow rates and pressures heat exchanger length and width are obtained so as to keep pressure loss at a specified value. Length Δx_m of the heat load segment *m* is calculated using OHTC derived from the local Nusselt number (Equation 26), and incremental pressure loss is calculated in a similar way. After convergence, the heat transfer area as well as length will be obtained.

6 Conclusions

The GMTD method was proposed for thermal-hydraulic analysis of heat exchangers with distributed physical properties. This method gives exactly the same result as the LMTD method, in the case that physical properties are all constant. For the case of a hot water supplier operating with supercritical carbon dioxide as heating media, GMTD was calculated, which is about 0.6 times less than LMTD. Moreover, experimental validation of the methodology was carried out using the supercritical CO_2 test loop. Empirical formulae for the local Nusselt number and local pressure loss factor were obtained using the GMTD method. Reproduction of temperature profiles was compared with measurements, in which excellent agreement was obtained. Based on the correlation developed, a design flow diagram was also developed for heat exchangers with distributed physical properties. In the case that OHTC is given, direct usage of the LMTD method was found to predict a smaller heat transfer area of heat exchangers with distributed physical properties in the present operating conditions. Therefore, we can safely conclude that the LMTD method may be substituted by the present GMTD method for the design of heat exchangers in general, and for the cases when distributed physical properties are anticipated, in particular.

Acknowledgement

This work was partly performed under the programme ‘Strategic Development of Technology for Efficient Energy Utilisation – Project of Fundamental Technology Development for Energy Conservation’ sponsored by NEDO.

Nomenclature

A	Heat transfer area	[m^2]
a	Heat transfer area per unit length of heat exchanger	[m]
AOHTC	Averaged Overall Heat Transfer Coefficient	[W/m^{2}K]
C^*	Heat conductance (=A_iU_i)	[W/K]
Cp	Specific heat	[J/kgK]
D_h	Hydraulic diameter	[m]
F	Function (Equation (22))	[W/m^{2}K]

f	Pressure loss coefficient	[–]
G	Mass flux	[kg/ m^{2}s]
GMTD	Generalised Mean Temperature Difference	[K]
h	Specific enthalpy	[W/kg]
K	$= mCp$	
L	Length of heat exchanger	[m]
LMTD	Logarithmic Mean Temperature Difference	[K]
MCHE	Microchannel heat exchanger	[–]
m	Mass flow rate	[kg/s]
N	Number of Thermal Unit (*NTU*)	[m]
Nu	Nusselt number ($=\alpha D_h/\lambda$)	[–]
OHTC	Overall Heat Transfer Coefficient	[W/m^{2}K]
ΔP	Pressure loss	[Pa]
Pr	Prandtl number	[–]
Q	Heat load	[W]
Re	Reynolds number ($=G\,D_h/\mu$)	[–]
s	Number of flow channel rows	[–]
T	Temperature	[K]
ΔT	Temperature difference between two fluids	[K]
Δ	Wall thickness	[m]
U	Overall heat transfer coefficient	[W/m^{2}K]
W	Mass flow of fluid	[kg/s]
Greek		
α	Heat transfer coefficient	[W/m^{2}K]
λ	Heat conductivity	[W/mK]
μ	Viscosity of fluid	[Pa · s]
ρ	Fluid density	[kg/m^3]
$\mathbf{\Delta}$	Increment	
Subscript		
i	Inlet, either 1(hot side) or 2(cold side)	
o	Outlet	
1	Hot side, constant of Nusselt formula	
2	Cold side, constant of pressure loss coefficient	

References

Hesselgreaves, J.E. (2001) *Compact Heat Exchangers, Selection, Design and Operation*, Pergamon, pp.1–2.

Ito, T., *et al*. (1990) *PROPATH: A Program Package for Thermo-physical Properties of Fluids*, Version 10.2, Tokyo, Japan: Corona Publishing Co.

Tsuzuki, N., Kato, Y. and Ishiduka, T. (2005) 'High performance printed circuit heat exchanger', *Heat SET 2005, Heat Transfer in Components and Systems for Sustainable Energy Technologies*, Grenoble, France, 5–7 April.

Utamura, M., Kato, Y., Nikitin, K., Ngo, T.L. and Ishizuka, T. (2006) 'Empirical correlations for thermal-hydraulic characteristics of compact heat exchangers with microchannels', *NTHAS5-N001, Proc. 5th Korea–Japan Symposium on Nuclear Thermal Hydraulics and Safety*, Jeju, Korea, 26–29 November.

Utamura, M. and Tamaura, Y. (2006) 'A solar gas turbine cycle with super-critical carbon dioxide as a working fluid', *Proc. ASME TURBO EXPO 2006, GT2006-90864*, Barcelona, Spain, 8–11 May.